Single vs. two photon microscopy for label free intrinsic tissue studies in UV light region

Vitalijs Zubkovs[a,b], Frédéric Jamme[a], Slavka Kascakova[c,d], Franck Chiappini[c,d], François Le Naour[c,d] and Matthieu Réfrégiers[a,*]

Fibrillar distribution in rat tail tendon and mice liver can be measured with optical methods. Two-photon excitation gives easy assessment of fibrotic collagen type I and II. Single photon deep ultraviolet (DUV) excitation imaging highlights all collagen types without discrimination. Their combination on the same tissue area provides a better overview of collagens in fibrillar diseases.

Introduction

Two-photon microscopy is a fast developing tool for cell biology and tissue diagnosis.[1-4] Its efficiency for imaging tissues in depth has been demonstrated and well recognized.[4] Due to its intrinsic non-linear nature it shines two type of signals, i) second harmonic generated (SHG) diffusion that brings easy localization of the non-centrosymmetric structures present in biological materials with specific information concerning their orientation; ii) using near infrared excitation, it allows to image the ultraviolet excited autofluorescence of biological samples[6] so called two-photon excitation fluorescence (TPEF). It is one of the possible methods to image label free biological samples with a great selectivity. SHG imaging can be applied for visualization of collagen[7], which is a key component of load-bearing tissues (bones, tendons, etc.) and the most abundant protein in human body (30% of proteins present in body mass[1]). Abnormalities in collagen development in several organs are often caused by a progression of inflammatory diseases and can be used as a pathological signature. SHG microscopy can be used to grade fibrosis in biological tissues. It should be highlighted that only fibrillar collagen types might be detected by SHG microscopy. Therefore globular collagen types do not give any SHG signal.[1,3]

On the other hand, ultraviolet excitable autofluorescent compounds can be imaged using single photon ultraviolet (UV) light in cells and tissues[8,9]. UV fluorescence microscopy in deep ultraviolet (DUV) range (200 – 300 nm) is an excellent tool for non-destructive qualitative specimen analysis.

Two-Photon Excitation Fluorescence (TPEF) microscopy can also be applied for autofluorescent imaging of endogenous compounds. But this technique cannot compete with monophotonic microscopies in discreteness of a recorded spectrum, despite same range lateral resolution.[10]

We describe for the first time the complementarities and synergies between ultraviolet single photon and two-photon excitation of autofluorescent compounds in tissues and compare the resolution and penetration depth of both modalities. Rat-tail as positive control and mice liver as unknown sample were studied and the potential of the combination was explored.

Methods and Materials

DUV Synchrotron light imaging

The full field synchrotron DUV imaging set-up is build around a Zeiss Axio Observer (Carl Zeiss, France) inverted microscope constructed with quartz-only optics. The white beam of DISCO beamline at Synchrotron SOLEIL[11] is monochromatized by an iHR320 (Jobin-Yvon Horiba, Longjumeau, France) before coupling with the entrance of a modified Zeiss Axio Observer Z1 (Carl Zeiss, Germany), monochromatic beam was chosen in order to determine composition of collagen in biological tissues exciting close to the 290 nm maximum, tryptophan and tyrosine were excited with the same excitation wavelength. A sharp dichroic mirror transmitting only above 300 nm (Omega Optical, Brattleboro, Vermont) reflected the incident light that was further focused onto the sample through a Zeiss Ultrafluar 100x (N.A. 1.25, glycerine immersion).[8] Emission was recorded with a Pixis 1024-BUV (Princeton Instruments, USA) camera after passing through a series of bandpass filters (Semrock, Rochester, USA). Fluorescence images were typically recorded in few seconds exposure (Table 1; DUV1 and DUV2). For bead's stack imaging, z scanning was performed with a PInano Z piezo slide scanner stage (PI, Germany). The whole system was controlled via µManager.[12]

Two-photon imaging microscopy

The samples were analyzed with a Nikon A1MP+ confocal microscope (NIKON, France). A tuneable Maï Taï XF Ti:Saphire mode-locked laser (SPECTRA PHYSICS, France) excited the sample between 710 and 920 nm through a 40x water immersion objective (N.A. 1.25, water immersion). Reflected second harmonic generated signal were detected at half the excitation wavelength with ad-hoc filters in front of the NDD GaAsP detectors. Excitation wavelength, acquisition time, and filters sets were chosen in order to maximize resolution and signal intensity in each channel (Table 1; rows IR1 to IR2).

Table 1. Microscopes acquisition parameters.

Number	Excitation wavelength (nm)	Emission filter (nm)	Image acquisition time (s)	Targeted compounds	Co-excited compounds
DUV1	290	327-353	5	Tryptophan	Tyrosine, Pyridoxine, Collagen Elastin, NADH, Pyridoxine
DUV2	290	412-438	5	Collagen	
IR1	810	399-414	32	Collagen (SHG)	
IR2	810	447-472	32	NADH, FAD (TPEF)	

Polystyrene beads

Monodisperse 220 nm polystyrene beads from the polybeads sampler kit III (Polysciences, France) were deposited and dried on a quartz coverslip before observation. They give a very convenient size distribution standard (220 ± 20 nm) for ultraviolet fluorescence microscopy due to the natural autofluorescence of polystyrene around 390 nm under DUV excitation.

Rat tail tendon

Rat tendons have been studied with different methods (SHG microscopy, Scanning Electron Microscopy (SEM), spectroscopy, chemical methods, etc.) and biochemical composition and their fibre organization is well characterized.[13-15] This tissue is rich in collagen type I fibrils making it an excellent sample for comparison of microscopy techniques. Rat-tail tendons were taken from Sprague-Dawley rats following EU 1986 procedures. Tendons were deposited on slides after physiological serum rinsing.

Mice liver histological sections

The study has been focused on liver samples from a mouse model fed on chow diet. The mice were grown in the animal facility of Institut André Lwoff (Villejuif, France). Mice were sacrificed after 5 weeks of breeding.

For SHG and DUV analysis fresh liver samples were fixed in formaldehyde and dehydrated in alcohol of increasing concentration up to absolute alcohol and finally immersed into toluene. Thereafter, the tissue was embedded in liquid paraffin, solidified and sectioned at 10, 20 µm with the microtome. Slices were mounted on quartz coverslips (thickness 0.17 mm) by addition of a drop of distilled water. In the standard sample preparation protocol, the human serum albumin is usually used. However using the UV excitation the addition of human serum albumin can lead to parasite signal. Therefore we excluded the albumin from preparation protocol. The tissues were well preserved but presented several cracks formed during the segmentation procedure.

Results and Discussion

Comparing resolutions

The usual way to compare the resolution of microscopes is to use calibrated nanobeads with fluorescent probes excited in the energy range of interest. In our case, for ultraviolet excitation, the best compromise we found was to use the natural fluorescence of polystyrene beads of known size.

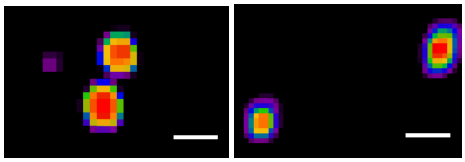

Figure 1. 220 nm polystyrene beads fluorescence imaging showing the resolving power of each microscopy technique. (**left**) 390 nm fluorescence after DUV excitation at 290 nm excitation. (**right**) TPEF image at 376 nm after IR 710 nm excitation. Scale bars 0.5 µm.

As seen on Fig. 1, the observed beads size after classic maximum likelihood estimation deconvolution is very close with both setups. Indeed, the natural confocal excitation provided by TPEF is compensated by the very low (290 nm) excitation wavelength of widefield DUV fluorescence microscopy. Therefore, for all the following images, we can directly compare the information content of TPEF and DUV images.

UV imaging of intrinsic tissues

Rat-tail

Before studying liver tissues samples, we wanted to compare the different modalities with a simple tissue, namely rat tail tendon which is known to be rich in type I collagen.[15] The imaging area was chosen randomly during the first acquisition. It should be mentioned that both imaging modalities are non-invasive for biological tissues and can therefore be applied in random order.

The abundance of types I, II collagen in rat tail tendon is

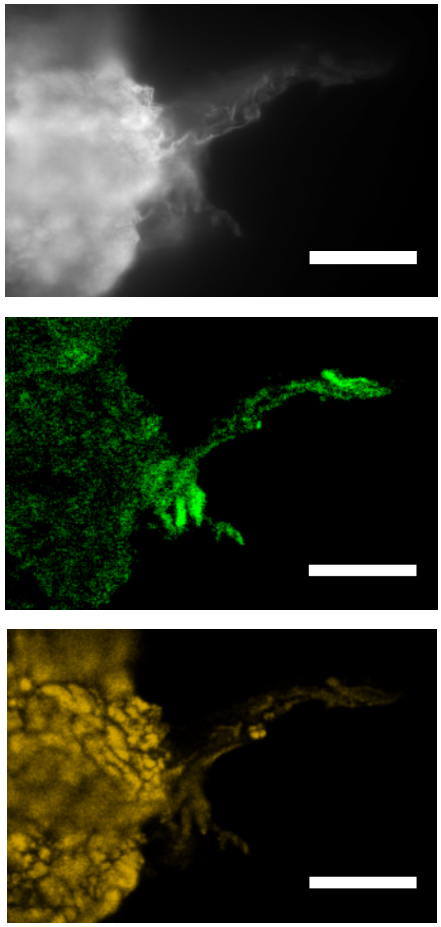

Figure 2. Rat-tail tendon multimodal imaging: Co-localized region of rat-tail tendon showing separate collagen fibres magnified. Collagen excitation at 290 nm in DUV, emission 412 - 438 nm. (**upper**) and collagen fibres visualization using SHG microscopy. **(middle)** and TPEF intrinsic fluorescence (447 - 472 nm) excited at 810 nm. **(bottom)** images. Scale bars 25 µm.

highlighted by SHG microscopy (*figure 2, middle*). In the tendon collagen architecture, two types of features can be highlighted: elongated, wave-like fibres and curved interwoven fibrils.[14] TPEF signal can be recorded simultaneously with SHG signal using higher wavelength bandpass filter sets, however, compared to single photon DUV excited fluorescence, TPEF excitation profile is less structured and selective.[16] It represents NADH and FAD distribution (table 1).

The same sample was transferred onto the DUV microscope for examination of collagen. On the figure 2, similarities in

organization of collagen bundles can be noticed between DUV fluorescence and SHG images. Separate collagen fibres bundles are well distinguishable, however, in cellular regions DUV fluorescence shows several other collagen fibres types which results in higher concentration (around 10% of all collagen types[15] in rat tail tendon).

Mice liver microscopy

As shown before on rat-tail tendon, collagen localization can be highlighted with DUV microscopy (Fig. 2) but cannot be typed.

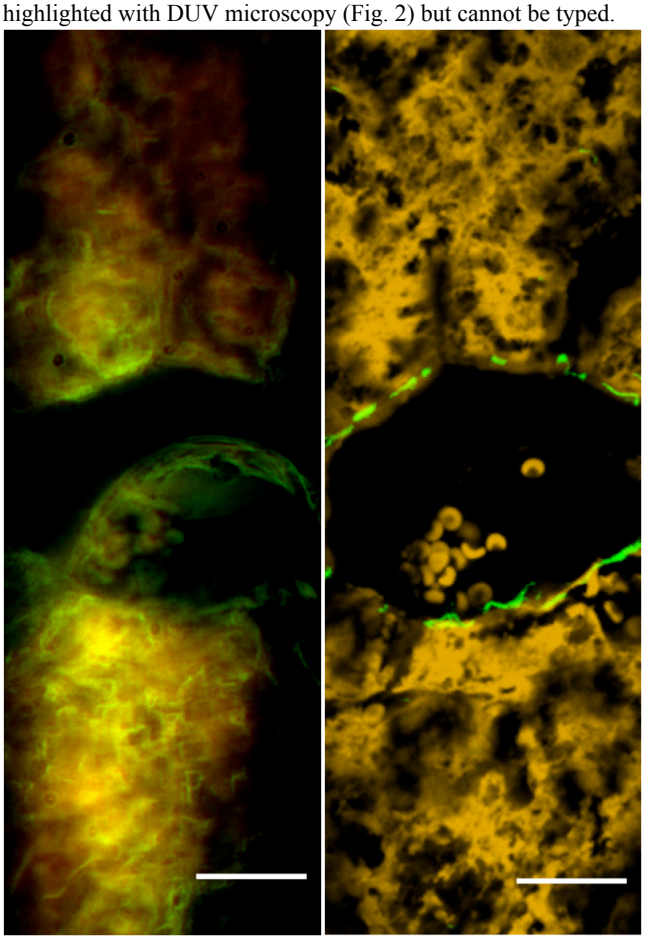

Figure 3. DUV fluorescence image (**left**), collagen is in green, amino acids in red and SHG image (green) merged with TPEF (yellow) (**right**) of healthy mice liver (excitation: 330 nm; emission: 412 – 438 nm; targeting regions of collagen localization). Scale bar 20 µm.

We observe collagen type I and II surrounding the central vein but also cells in DUV while in SHG only around the vein (Fig. 3). Ultraviolet excited fluorescence (either two-photon or single photon, yellow in Fig. 3) permits also to visualize hematocytes that remained trapped inside the vein, only DUV microscopy shows the network of fibres surrounding those cells.

DUV microscopy illustrates the distribution of endogenous compounds in the liver tissue. The filters have been chosen close to regions of fluorescence maxima of tryptophan, collagen and elastin. The band pass filter at 327 – 353 nm (excitation at 290 nm) was used to visualize tryptophan occurrence in the biological sample (Fig. 3). It reveals protein distribution in the liver with different pathologies. The differences in signal intensities between two channels (red filters at 327 – 353 nm and green at 412 – 438 nm) allow the detection of collagen abundance.

Collagen type IV forms a structural basis of cell membranes. Because it is a globular protein, it can be imaged by DUV microscopy only, not by SHG.[3] Therefore, DUV fluorescence imaging provides deeper knowledge concerning collagen repartition in tissues (Fig. 3).

Collagen fibres develop mostly in vascular regions. Collagen fibres have spring-like structures that are randomly oriented surrounding cell membranes. But close to veins or arteries collagen fibres are co-directed around the tubular objects (Fig. 3).

Conclusions

Two-photon microscopy found a broad range of applications in biology, for example, multi-photon excitation imaging of neuron activity, cancer research studies of angiogenesis, metastasis and embryo development visualization.[10] On the other hand, Deep UV light (200-300 nm) and near UV light (300-400 nm) are used for excitation of many endogenous compounds, which are responsible for native tissue fluorescence. The endogenous fluorophores present in most biological tissues are: NADH coenzymes which is present in mitochondria, chloroplasts, peroxisomes, cytosol and is involved in cellular metabolism, presents an excitation maxima at 260 and 345 nm[9,17], aromatic autofluorescent amino acids: tryptophan (excitation maxima 220 and 277 nm), tyrosine (274 nm), phenylalanine (257 nm) compose many proteins. Furthermore, flavins, collagen, elastin, FAD and lipopigments are endogenous chromophores in tissues under UV light excitation. [9,18]

Development of new methods for liver pathological tests is on front line of actuality in many known researches. SHG microscopy has high potential for characterization of fibrotic stages in liver and was approved the Fibrosis-Metavir test[3]. Moreover, it has been shown that collagen fibres detection in liver by non-linear microscopy provides better sensitivity compared to conventional staining methods.[19] Combination of SHG and synchrotron light excitation autofluorescence microscopies for biological tissue analysis has not been reported in any other study. Therefore, this research work has a significant value not only as a tool for the characterization of pathological disorders, but also demonstrates the compatibility of these techniques for analyzing the same sample. While SHG permits a fine localization and quantification of fibrillar collagen type I and II, DUV fluorescence microscopy images all collagen crosslinks without discrimination. While this loss in selectivity could be considered as a disadvantage, it may also be seen as an advantage because comparison between DUV and SHG images permits to localize collagens of other types than I and II.

Due to the potential presented for liver tissues fibrillar characterization, the mentioned microscopy methods could be applied to study pathological disorder caused by non-alcoholic fatty liver disease (NAFLD). Those disorders are expressed in an unordinary accumulation of lipid droplets in the liver of non-alcoholic patients.[20] NAFLD is classified between simple steatosis (fatty liver) and non-alcoholic steatohepatitis (NASH). The histopathological spectrum of NAFLD extends from steatosis through NASH to advanced fibrosis, cirrhosis and hepatocellular carcinoma (HCC). While steatosis refers to lipids accumulation, the key factor concurs to favour NASH are oxidative stress culminating with liver injury and inflammation.[21] It has been

shown that the simple hepatic steatosis confers a long-term prognosis. It is a process reversible, considered innocuous in its pure form. Indeed patients without evidence of NASH rarely progressed to cirrhosis[22,23], whereas the disease progression occurs in 43% of patients with NASH, and progression to cirrhosis may occur in 28% of these cases[23,24]. In addition, HCC has long been described to arise on a cirrhotic liver. Recent data however show that some patients with NASH can progress to HCC bypassing the stage of cirrhosis[25]. Therefore, NASH is now emerging as a leading risk factor owing to the epidemic of obesity and type 2 diabetes mellitus becoming major public health problem worldwide. Despite the major public health concern of NAFLD, it is currently impossible by the usual histological methods to identify at early stage patients that will progress from steatosis to NASH. This justifies the need of new methods to quantitatively assess the early biochemical changes related to this pathology.

At present, the gold standard for the diagnosis of liver pathology is liver biopsy. These liver probes are analyzed mainly by visual inspection after appropriate staining protocols. Although rich on information, from the clinical point of view, histopathology of liver is prone to intra- and inter-observer variability, which can yield poor reproducibility even when performed by experts. In the study of El-Badry et al.[26], 4 pathologists assessed the features of NAFLD/NASH and a strong disagreement was found for all parameters including the overall diagnosis. Evaluation of NAFLD is therefore strongly observer-dependent and seems weakly reproducible. The incapacity of objectively assess the NASH and identify at an early stage patients that will progress from steatosis to NASH justifies the need of new methods to quantitatively assess the biochemical changes related to this pathology. Recently, joint application of time-of-flight Secondary Ion Mass Spectrometry, DUV Microspectroscopy and infrared microspectroscopy for lipid, protein, sugar and nucleic acid mapping on liver samples has been developed.[1,27] Early studies showing SHG microscopy as a tool for liver-pathology examination, were reported.[28,29] Since then, several research groups assessed the method as a perspective technique bringing more sensitive results than conventional fibrosis scoring methods[3,9] and proposed a quantification method.[20,30] Because SHG microscopy presents perspectives as a fast, non-destructive, quantitative technique, which eliminates human factors in liver analysis procedure, its combination with DUV single photon fluorescence microscopy looks even more promising.

Notes and references

[a] *DISCO Beamline, Synchrotron SOLEIL, F-91192 Gif sur Yvette, France. Fax: 33 1 69359456; Tel: +33 1 69359655; E-mail: matthieu.refregiers@synchrotron-soleil.fr*

[b] *actual adress: EPFL / STI – IBI – STI / LBP - CH – 1015 Lausanne, Switzerland*

[c] *Inserm U785, F-94800 Villejuif, France*

[d] *Univ. Paris-Sud 11, UMR-S785, F-94800 Villejuif, France*

Acknowledgments

Vitalijs Zubkovs is supported by ERASMUS MUNDUS student grant. We acknowledge Synchrotron SOLEIL support through projects #20100064, 201000181, 20100949 and 20110131.

1. G.A. Di Lullo, S.M. Sweeney, J. Körkkö, L. Ala-Kokko and J.D. San Antonio, *Journal of Biological Chemistry*, 2001, **277**, 4223–4231.
2. P. Campagnola, M. Wei, A. Lewis and L.M. Loew, *Biophysical Journal*, 1999, **77**, 3341-3349.
3. L. Gailhouste, Y. Le Grand, C. Odin, D. Guyader, B. Turlin, F. Ezan, Y. Désille, T. Guilbert, A. Bessard, C. Frémin, N. Theret, and G. Baffet, *Journal of Hepatology*, 2010, **52**, 398–406.
4. P. Campagnola, A. Millard, M. Terasaki, P.E.. Hoppe, C.J. Malone and W.A. Mohler, *Biophysical Journal*, 2002, **81**, 493-508.
5. J. A. Palero, H. S. de Bruijn, A. van der Ploeg van den Heuvel, H. J. C. M. Sterenborg, and H. C. Gerritsen, *Biophysical Journal*, 2007, **93**, 992–1007.
6. G. Filippidis, E. J. Gualda, M. Mari, K. Troulinaki, C. Fotakis, and N. Tavernarakis, *Micron*, 2009, **40**, 876–880.
7. X. Chen, O. Nadiarynkh, S. Plotnikov, and P. J. Campagnola, *Nature Protocols*, 2012, **7**, 654–669.
8. F. Jamme, S. Villette, A. Giuliani, V. Rouam, F. Wien, B. Lagarde, and M. Refregiers, *Microsc Microanal*, 2010, **16**, 507–514.
9. F. Jamme, S. Kascakova, S. Villette, F. Allouche, S. Pallu, V. Rouam, and M. Refregiers, *Biology of the Cell*, 2013, **105**, 277-288.
10. W. R. Zipfel, R. M. Williams, and W. W. Webb, *Nat Biotechnol*, 2003, **21**, 1369–1377.
11. A. Giuliani, F. Jamme, V. Rouam, F. Wien, J.-L. Giorgetta, B. Lagarde, O. Chubar, S. Bac, I. Yao, S. Rey, C. Herbeaux, J.-L. Marlats, D. Zerbib, F. Polack, and M. Refregiers, *J Synchrotron Rad*, 2009, **16**, 835–841.
12. A. Edelstein, N. Amodaj, K. Hoover, R. Vale, and N. Stuurman, *Current protocols in molecular biology*, 2010, **92**, 14.20.1–14.20.17.
13. A. A. de Aro, B. de Campos Vidal, and E. R. Pimentel, *Micron*, 2012, **43**, 205–214.
14. P. P. Provenzano and R. Vanderby Jr., *Matrix Biology*, 2006, **25**, 71–84.
15. T. A. Theodossiou, C. Thrasivoulou, C. Ekwobi, and D. L. Becker, *Biophysical Journal*, 2006, **91**, 4665–4677.
16. W. Zipfel, R. Williams, R. Christie, A. Nikitin, B. Hyman, and W. Webb, *Proc. Nat. Acad. Sci. U.S.A.*, 2003, **100**, 7075–7080.
17. M. R. Kasimova, J. Grigiene, K. Krab, P.H. Hagedorn, H. Flyvbjerg, ¨.E. Andersen and I.M. Moller, *The Plant Cell*, 2006, **18**, 688–698.
18. A. G. Wagnières, W. M. Star, and B. C. Wilson, *Photochem Photobiol*, 1998, **68**, 603–632.
19. D. C. S. Tai, N. Tan, S. Xu, C. H. Kang, S. M. Chia, C. L. Cheng, A. Wee, C. L. Wei, A. M. Raja, G. Xiao, S. Chang, J. C. Rajapakse, P. T. C. So, H.-H. Tang, C. S. Chen, and H. Yu, *J. Biomed. Opt.*, 2009, **14**, 044013.
20. P. Angulo, *Hepatology*, 2010, **51**, 373–375.
21. C. P. Day and O. F. James, *Gastroenterology*, 1998, **114**, 842-845.
22. M.R. Teli, O.F. James, A.D. Burt, M.K. Bennett and C.P. Day, *Hepatology*, 1995, **22(6)**, 1714-1719.
23. C.A. Matteoni, Z.M. Younossi, T. Gramlich, N. Boparai, Y.C. Liu and A.J. McCullough, *Gastroenterology*, 1999, **116(6)**, 1413-1419.
24. R.G. Lee, *Hum. Pathol.*, 1989, **20 (6)**, 594-598.
25. K. Yasui, E. Hashimoto, Y. Komorizono, K. Koike, S. Arii, Y. Imai, T. Shima, Y. Kanbara, T. Saibara, T. Mori, S. Kawata, H. Uto, S. Takami, Y. Sumida, T. Takamura, M. Kawanaka and T. Okanoue, *Clin. Gastroenterol. Hepatol.*, 2011, **9(5)**, 428-433.
26. A.M. El-Badry, S. Breitenstein, W. Jochum, K. Washington, V. Paradis, L. Rubbia-Brandt, M.A. Puhan, K. Slankamenac, R. Graf and P.A. Clavien, *Ann Surg*, 2009, **250(5)**, 691-697.
27. V. W. Petit, M. Refregiers, C. Guettier, F. Jamme, K. Sebanayakam, A. Brunelle, O. Laprevote, P. Dumas, and F. Le Naour, *Anal. Chem.*, 2010, **82**, 3963–3968.
28. R. Bataller and D.A. Brenner, *Journal of clinical investigation*, **115**, 209–218.
29. G. Cox, E. Kable, A. Jones, I. Fraser, F. Manconi, and M. D. Gorrell, *Journal of Structural Biology*, 2003, **141**, 53–62.
30. T. Guilbert, C. Odin, Y. Le Grand, L. Gailhouste, B. Turlin, F. Ezan, Y. Désille, G. Baffet, and D. Guyader, *Optics Express*, 2010, **18**, 25794–25807.